

High-performance optofluidic membrane microreactor with a mesoporous CdS/TiO₂/SBA-15@carbon paper composite membrane for the CO₂ photoreduction

Rong Chen^{a,b*}, Xiao Cheng^{a,b}, Xun Zhu^{a,b**}, Qiang Liao^{a,b}, Liang An^c, Dingding Ye^{a,b}, Xuefeng He^{a,b}, Zhibin Wang^{a,b}

^a Key Laboratory of Low-grade Energy Utilization Technologies and Systems (Chongqing University), Ministry of Education, Chongqing 400030, China

^b Institute of Engineering Thermophysics, Chongqing University, Chongqing 400030, China

^c Department of Mechanical Engineering, The Hong Kong Polytechnic University, Hung Hom, Kowloon, Hong Kong, China

*Corresponding author. Tel.: 86-23-65103119; fax: 86-23-65102474; e-mail: rchen@cqu.edu.cn

**Corresponding author. Tel.: 86-23-65102474; fax: 86-23-65102474; e-mail: zhuxun@cqu.edu.cn

Abstract

In this study, a novel mesoporous CdS/TiO₂/SBA-15@carbon paper composite membrane was developed to enhance the visible-light responsive CO₂ photoreduction in an optofluidic membrane microreactor. The microscopic morphological and pore volume characterizations indicated that the incorporation of the mesoporous SBA-15 into the membrane development could greatly improve the specific surface area and pore volume. The optofluidic membrane microreactor with the newly-developed composite membrane was evaluated in terms of the methanol concentration and yield. Experimental results showed that the optofluidic membrane microreactor with mesoporous CdS/TiO₂/SBA-15@carbon paper composite membrane yielded much better performance than did the one without the mesoporous SBA-15. For a given total amount of TiO₂/SBA-15 in the composite membrane, too high dosage of TiO₂ in

the composite membrane caused the reduction in the specific surface area and pore volume, thereby lowering the photocatalytic performance. In addition, it was found that the methanol concentration and yield firstly increased and then decreased with increasing the liquid flow rate. The increase of both the light intensity and NaOH concentration was able to enhance the methanol generation. The obtained results fully demonstrate the superiority of the newly-developed CdS/TiO₂/SBA-15@carbon paper composite membrane for enhancing the CO₂ photoreduction.

Keywords: Mesoporous SBA-15; CdS/TiO₂/SBA-15@carbon paper composite membrane; Optofluidic membrane microreactor; CO₂ photoreduction

1. Introduction

Every year a huge amount of fossil fuels is consumed to meet the rapid economic growth. Meanwhile, carbon dioxide (CO₂), as the main greenhouse gas source, is also emitted into the atmosphere. Under this circumstance, rapid depletion of fossil fuels and the resultant greenhouse gas emissions have led to serious energy crisis and environmental problems. To simultaneously address these two critical issues, the conversion of CO₂ into fuels has become an important way for sustainable energy and environmental development [1, 2]. Among existing CO₂ conversion technologies, the CO₂ photoreduction by solar energy has been regarded as one of the most promising approaches [3, 4], because not only the solar energy can be utilized but also the CO₂ can be converted into liquid or gas solar fuels.

Over the past decades, to improve the production of solar fuels by the CO₂ photoreduction, various photocatalysts have been developed to improve photocatalytic CO₂ conversion [5-7]. TiO₂ has attracted much attention due to its high stability and durability [8]. Nevertheless, pure TiO₂ has some serious disadvantages that restrict its wide applications. One of them is that the employed TiO₂ nanoparticles are usually agglomerated to form clusters. The resulting low specific surface area deteriorates the performance [9]. For this reason, mesoporous materials and structures with large specific surface area and pore volume have been utilized such that high specific surface area and highly-dispersed TiO₂ nanoparticles are achieved to improve the photocatalytic activity [10-13]. Yang et al. [14] embedded nano-titania particles into mesoporous SBA-15 to form TiO₂/SBA-15 composites, by

which higher photo-degradation ability for methylene blue than commercial pure TiO₂ (Degussa, P25) and proper pore diameter were obtained. Li et al. [15] synthesized a series of TiO₂@SBA-15 composites through a facile sol-gel method, and they found that the SBA-15 retained the mesoporous structure and TiO₂ particles were uniformly dispersed. The prepared Pt/TiO₂@SBA-15 composites showed superior performance than did the Pt/TiO₂ catalysts for the hydrogenation of benzaldehyde. Yang et al. [16] prepared mesoporous TiO₂/SBA-15, Cu/TiO₂ and Cu/TiO₂/SBA-15 composite photocatalysts by the sol-gel method for the CO₂ photoreduction to methanol. A high methanol yield of 627 μmole/g-cat·h was achieved. Therefore, the mesoporous materials have the promising potential to improve the performance of the CO₂ photoreduction. In addition to the low specific surface area, another drawback using pure TiO₂ is that the electron/hole pairs can only be photo-excited under the UV light stimulation, which only accounts for 3~5% of sunlight. To broaden the light responsive range and improve the solar energy utilization efficiency, various visible-light responsive photocatalysts have been developed [17]. Cadmium sulfide (CdS) has been considered as one of the most attractive semiconductors due to its proper band gap and band position [18]. As a result, combining CdS with TiO₂ could efficiently extend the light responsive spectra. Moreover, Lunawat et al. [19] dispersed the nanocrystallites of CdS into mesoporous SBA-15, by which a higher activity for water-splitting than bulk CdS was obtained. This is a successful attempt to incorporate the mesoporous material into the visible-light responsive photocatalyst. Although the combinations of the semiconductor composites, such as TiO₂/SBA-15,

CdS/SBA-15 and CdS/TiO₂, have been studied for various purposes, the ternary hybrid CdS/TiO₂/SBA-15 has not been reported for the CO₂ photoreduction application. It can be foreseen that the ternary hybrid CdS/TiO₂/SBA-15 is able to show good activity toward the CO₂ photoreduction.

It should be noted that the photoreactor design is also of importance to improve the performance of the CO₂ photoreduction. However, the problems of low surface-area-to-volume ratio, non-uniform light distribution and poor light utilization efficiency are usually encountered in existing photoreactors. Recently, the combination of microfluidics and optics creates a new interdisciplinary research area, so-called optofluidics, which has a distinct feature of fluids, light and their interactions. Such combination offers several advantages of large surface-area-to-volume ratio, uniform light distribution, enhanced mass transfer and fine flow control. Hence, optofluidics based microreactors have exhibited superior performance in various photocatalytic processes, such as water-splitting [20], wastewater treatment [21] and CO₂ photoreduction by optofluidic planar microreactor [22]. As one of the important microreactor types, membrane microreactors for various applications have also been widely studied [23-25]. More recently, we incorporated optofluidics into the membrane reactor technology to newly develop an optofluidic membrane microreactor for the CO₂ photoreduction and the pretty good performance was achieved [26]. Inspired by this idea along with the merits offered by the mesoporous materials, in this work, we added the mesoporous SBA-15 into CdS/TiO₂ to develop a ternary hybrid CdS/TiO₂/SBA-15@carbon paper composite membrane

for the optofluidic membrane microreactor toward the visible-light responsive CO₂ photoreduction. The morphology, BET surface area, pore volume and spectrum of the prepared composite membranes were characterized. Since methanol is one of the basic products in the CO₂ photoreduction, which can be used in direct methanol fuel cells [27], only the methanol concentration was measured to estimate the methanol yield in this work, with which the performance of the developed membrane microreactor could be evaluated. In addition, the effects of the design and operating parameters were also visited.

2. Materials and methods

2.1 Preparation of the CdS/TiO₂/SBA-15@carbon paper composite membrane

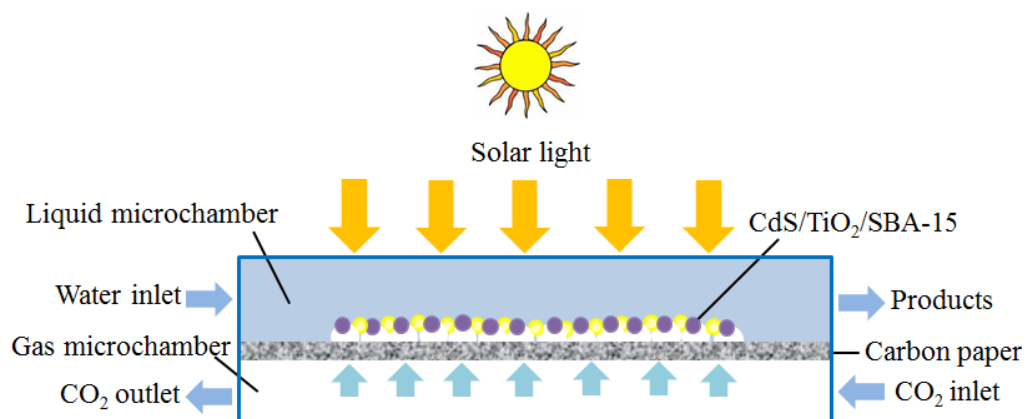
The visible-light responsive CdS/TiO₂/SBA-15@carbon paper composite membrane is the key component in the development of the optofluidic membrane microreactor. In this work, the preparation of this composite membrane included four steps. Step one was the preparation of the TiO₂/SBA-15 composite. In this process, 12 g commercial TiO₂ powders (Degussa P25) were slowly poured into 120 mL DI water with 0.4 mL acetylacetone (Sigma-Aldrich) under continuously magnetic stirring. 0.2 mL Triton X-100 (Sigma-Aldrich) was added to facilitate the spreading of the colloid. 2.4 g polyethylene glycol 2000 (Chengdu Kelong, China) was then added and the colloid was magnetically stirred for 12 h. For the preparation of SBA-15, 1 g mesoporous silica SBA-15 (Zhejiang Nasenmei Nano material Co.) was dissolved in 10 mL ethanol under vigorous stirring for 12 h, and then the prepared TiO₂ colloid

were added into the SBA-15 solution. The mixture was then continuously stirred over one night. By the impregnation, the TiO₂ nanoparticles can be deposited into and onto the mesoporous structure of SBA-15. The second step was the coating of TiO₂/SBA-15 onto the carbon paper. Here, the as-received carbon paper (Shanghai Hesun, China) was firstly covered by a paper mask with a hole of 1 cm × 1 cm = 1 cm². The prepared TiO₂/SBA-15 mixture was sprayed onto the carbon paper. After removing the paper mask, the TiO₂/SBA-15 coated carbon paper was dried under room temperature and then calcined at 550 °C for 2 h in the air environment. The third step was the hydrophobic treatment. In this step, the poly-tetrafluoroethylene (PTFE) solution was sprayed onto the other side of the carbon paper without the coated photocatalysts followed by the calcination at 360 °C for 1 hour in air. The PTFE dry weight was about 1 mg/cm². By doing this, efficient separation of liquid phase from gas phase could be ensured. The last step was the quantum-dots sensitization. To do this, cadmium sulfide (CdS) was coated onto the TiO₂/SBA-15 surface by the impregnation method [28]. In brief, two aqueous solutions were used including Cd(NO₃)₂·4H₂O and Na₂S·9H₂O. The photocatalyst-coated side of the carbon paper was immersed into Cd(NO₃)₂·4H₂O solution for 10 min followed by washing with distilled water and then immersed into Na₂S·9H₂O solution for 10 min followed by washing with distilled water again, forming a cycle. After 5 cycles, the prepared composite membrane was swept with N₂ stream and baked at 100 °C for 10 min. So far, the visible-light responsive CdS/TiO₂/SBA-15@carbon paper composite membrane was achieved. In this work, two CdS/TiO₂/SBA-15@carbon paper

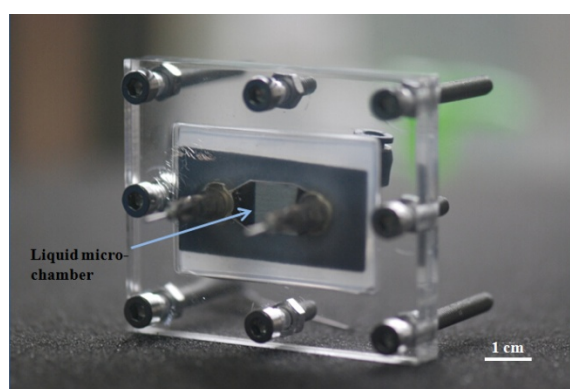
composite membranes were prepared by varying the weight ratio of TiO₂ in the TiO₂/SBA-15. One was 20% of TiO₂, termed as CdS/20 wt% TiO₂/SBA-15, the other was 40% of TiO₂, termed as CdS/40 wt% TiO₂/SBA-15. Besides, the CdS/TiO₂@carbon paper composite membrane was also prepared for comparison. The total loadings of all samples were about 2 mg/cm².

2.2 Design of the optofluidic membrane microreactor

As mentioned earlier, the reactor design is another important factor affecting the performance. In this study, based on the developed composite membranes, an optofluidic membrane microreactor was developed, which was similar to our previous work [26]. As illustrated in Fig. 1a, the developed optofluidic membrane microreactor consisted of a liquid microchamber, a composite membrane and a gas microchamber. The assembled membrane microreactor is shown in Fig. 1b. The dimensions of the reaction microchamber were 1 cm×1 cm×80 μm, providing the merits of high surface-area-to-volume ratio, uniform light distribution and enhanced mass transfer. Besides, the hydrophobic treatment of these composite membranes ensured the separation of the gas phase from the liquid phase, by which the reactants of gas CO₂ and liquid phase could be independently supplied into the microreactor, respectively. Such design can also efficiently eliminate the mass transfer resistance associated with the gas/liquid interface and liquid film encountered in conventional slurry reactors.



(a)



(b)

Fig. 1 (a) Schematic and (b) photo of the optofluidic membrane microreactor.

2.3 Experimental setup

The CO₂ photoreduction system mainly consisted of five components: a syringe pump, a CO₂ gas cylinder, an optofluidic membrane microreactor, a simulated sunlight source and a collection vessel. In this work, different NaOH aqueous solutions were pumped into the liquid microchamber by a syringe pump (Pump 33, Harvard). 99.99% CO₂ gas was supplied into the gas microchamber through a gas volumetric flowmeter (Omega, FMA-2617A-1). The flow rate of CO₂ was maintained

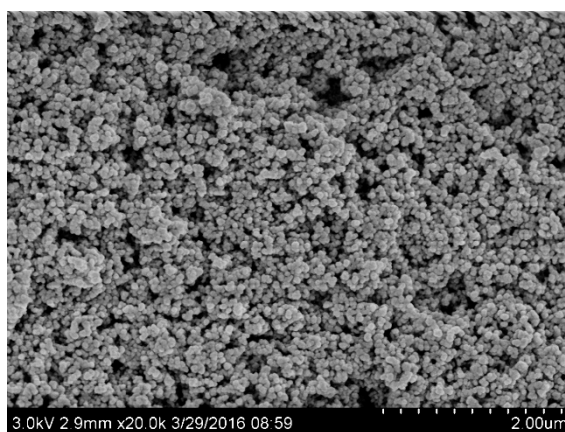
at 25 mL/min in all experiments. A xenon lamp (CEL-HXF300, CEAULIGHT, China) was employed to simulate the sunlight. The light intensity was controlled by adjusting the distance between the microreactor and xenon lamp, and measured by a FZ radiometer (FZ-A, Photoelectric Instrument Factory of Beijing Normal University, China). An electric fan was used to blow air to the microreactor for the cooling effect such that the temperature effect on the performance of the microreactor can be eliminated. In this work, we measured the methanol concentration to estimate the methanol yield so that the performance of the developed microreactor could be assessed. The products were analyzed by a GC (GC-2010 plus, Shimadzu) equipped with an FID detector using a 30-m Wax capillary column. Blank tests were also conducted by feeding inert gas of N₂ and no methanol was detected. All experiments were repeated at least three times under room temperature of about 15 °C.

3. Results and discussion

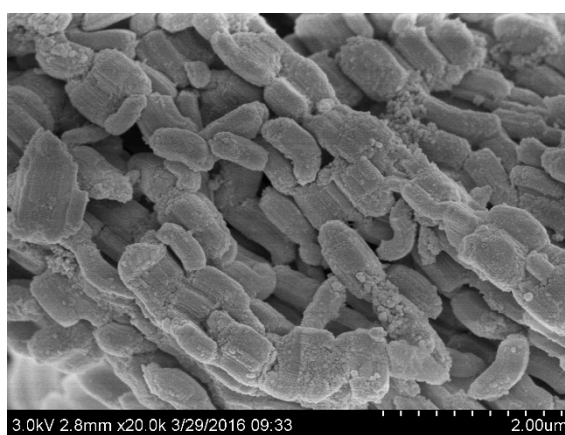
3.1 Characterization of the photocatalysts

The prepared composite photocatalysts were characterized by the field-emission scanning electron microscope (FE-SEM, Hitachi S4800) and the results are presented in Fig. 2. As seen, for pure TiO₂, the nanoparticles were easily agglomerated to form clusters. The pore size ranged from dozens of nanometers to one micrometer. However, when adding the mesoporous silica of SBA-15, the morphologies were significantly changed. For 20 wt% TiO₂/SBA-15, the morphology of SBA-15 was

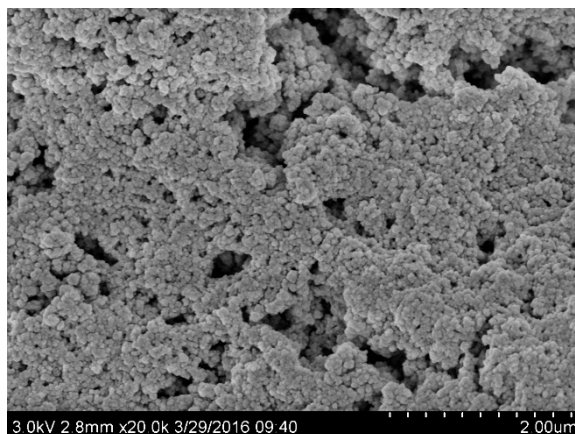
retained and TiO₂ nanoparticles were uniformly deposited into and onto the surface of SBA-15. Since the TiO₂ loading was low, the mesoporous structure of SBA-15 was remained with a significant amount of meso pores arising from the SBA-15 nature and macro pores between the SBA-15 particles. Such porous structure could enhance the mass transfer and adsorption, photon transfer and light scattering in this layer. As the TiO₂ loading increased to 40 wt%, those meso and macro pores were occupied by TiO₂ nanoparticles, making it become rather dense. In this case, the mass and photon transfer might be resisted. Hence, from the point view of the microscopic morphology, the 20 wt% TiO₂/SBA-15 was expected to be favorable for the CO₂ photoreduction.



(a)



(b)



(c)

Fig. 2 The FE-SEM images of (a) TiO_2 , (b) 20 wt% $\text{TiO}_2/\text{SBA-15}$ and (c) 40 wt% $\text{TiO}_2/\text{SBA-15}$.

In this work, diffuse reflectance UV-Visible absorption spectra (UV-Vis) was utilized to assess the visible-light response of the $\text{CdS}/\text{TiO}_2/\text{SBA-15}$ @carbon paper composite membranes, and the results are shown in Fig. 3. It can be seen that either CdS/TiO_2 or $\text{CdS}/\text{TiO}_2/\text{SBA-15}$ all demonstrated remarkable visible-light response. The main absorption regions of them were all below the wavelength of 540 nm. After adding the mesoporous silica of SBA-15, the absorption domain of $\text{CdS}/\text{TiO}_2/\text{SBA-15}$ was clearly increased in the range of 400~540 nm. This may be due to the fact that the mesoporous SBA-15 allowed more CdS to be formed and enhanced the reflection and scattering of light. It is also observed that the absorption with the 20 wt% TiO_2 was higher than that of the 40 wt% TiO_2 . This may be because too high TiO_2 dosage blocked some meso and macro pores, which decreased the photon transfer.

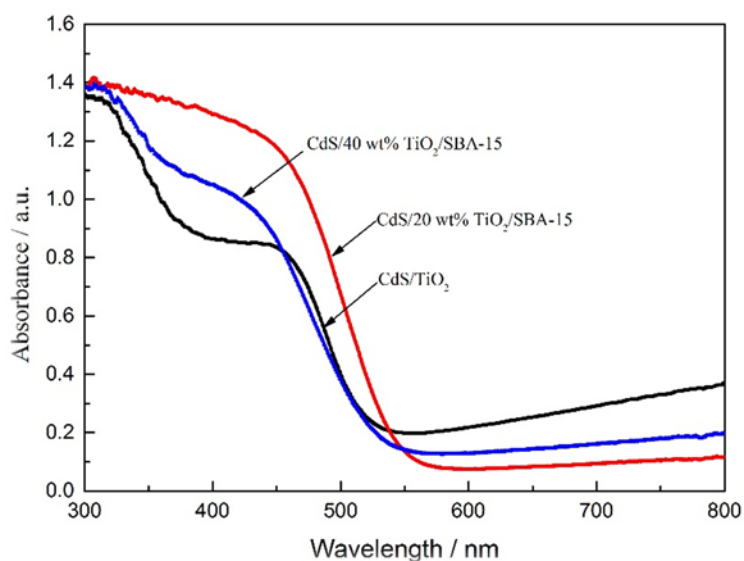


Fig. 3 The UV-Vis spectra of the prepared composite membranes.

Table 1 lists the textural properties of TiO_2 , SBA-15 and $\text{TiO}_2/\text{SBA-15}$ with various TiO_2 dosages determined by the nitrogen adsorption/desorption isotherms. The BET surface area, pore volume and pore diameter were all derived from the N_2 -adsorption data. Clearly, pure TiO_2 showed the smallest BET surface area, which was much lower than the SBA-15. For the $\text{TiO}_2/\text{SBA-15}$, the addition of TiO_2 into SBA-15 decreased the BET surface area in comparison to SBA-15. This is because when adding the TiO_2 nanoparticles, some intrinsic pores of SBA-15 were blocked, leading to the lowered BET surface area. Although the BET surface areas of the $\text{TiO}_2/\text{SBA-15}$ samples were lower than that of SBA-15, they were still much higher than that of pure TiO_2 . In addition, it could also be found that the increase of the TiO_2 dosage resulted in the lowered BET surface area. It is understood that more addition of the TiO_2 nanoparticles might cause more intrinsic pores of SBA-15 to be blocked. Under such

a circumstance, the BET surface area accordingly became lower with increasing the TiO₂ dosage. Because of the same reason, increasing the TiO₂ dosage in the composite membrane led to the decreased pore volume. On the contrary, it is interesting to find that the average pore diameter increased with the increasing of the TiO₂ dosage. The average pore diameter increased from 8.045 nm of SBA-15 to 8.428 nm of 40 wt% TiO₂/SBA-15. This may be caused by the contribution of the naked titania character in the photocatalysts with the increase of the TiO₂ dosage [29]. In a word, the mesoporous TiO₂/SBA-15 photocatalysts showed better textural properties than did pure TiO₂.

Table 1 Textural properties

Sample	BET surface area (m ² /g)	Pore volume (cm ³ /g)	Average pore diameter (nm)
TiO ₂	76.8	0.367	18.67
SBA-15	565.8	1.138	8.045
20 wt% TiO ₂ /SBA-15	422.5	0.863	8.175
40 wt% TiO ₂ /SBA-15	369.6	0.779	8.428

3.2 Performance evaluation

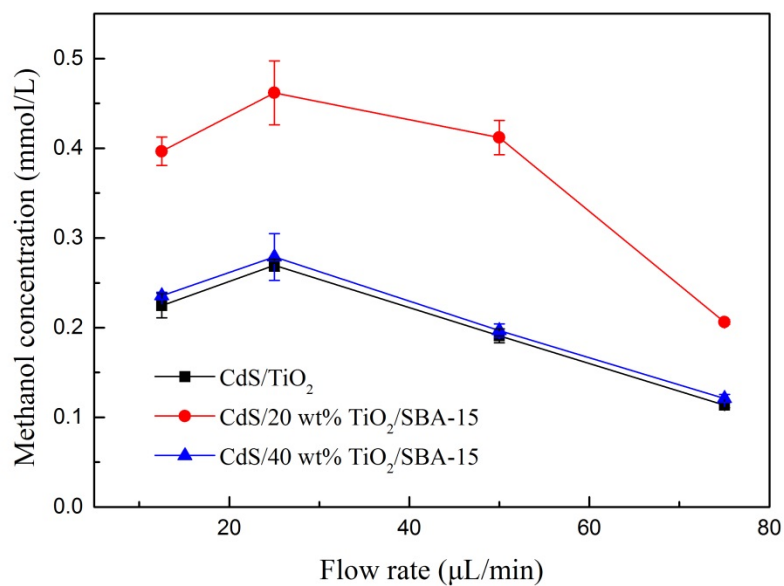
In this study, the microreactor was operated in an alkaline environment, which had four advantages. First of all, CO₂ could dissolve more in the alkaline environment than pure water. Second, OH⁻ ions could act as hole-scavengers in aqueous solution such that the recombination of hole-electron pairs can be restrained, which is extremely meaningful for the photocatalytic process [30]. Third, because the photo-generated holes could be scavenged by the OH⁻ ions, the photo-corrosion of

CdS would be weakened, allowing CdS to be more stable [31]. Fourth, high methanol selectivity could be obtained for the TiO₂-containing mesoporous photocatalysts in alkaline environment [32]. Because the liquid flow rate, light intensity and NaOH concentration play vital roles in the CO₂ photoreduction to methanol, the developed visible-light responsive CdS/TiO₂/SBA-15@carbon paper composite membrane was assessed by measuring the methanol concentration at the outlet of the optofluidic membrane microreactor to estimate the methanol yield under different liquid flow rates, light intensities and NaOH concentrations.

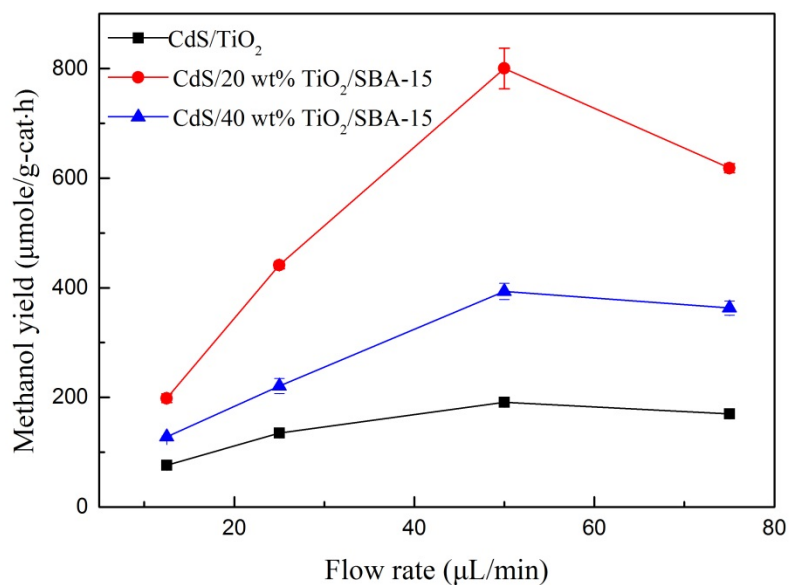
3.2 Effect of the liquid flow rate

Figure 4 compares the performances of the optofluidic membrane microreactors with CdS/TiO₂/carbon paper, CdS/20 wt% TiO₂/SBA-15/carbon paper and CdS/40 wt% TiO₂/SBA-15/carbon paper composite membranes under the liquid flow rate ranging from 12.5 μ L/min to 75 μ L/min. The light intensity and NaOH concentration were maintained at 100 mW/cm² and 0.05 M, respectively. It can be seen that the optofluidic membrane microreactor with the incorporation of SBA-15 into the composite membrane was able to yield higher methanol concentration than did the CdS/TiO₂. At the liquid flow rate of 25 μ L/min, the methanol concentrations of the CdS/20 wt% TiO₂/SBA-15 and CdS/40 wt% TiO₂/SBA-15 were 0.46 mmol/L and 0.28 mmol/L, respectively, while it was 0.27 mmol/L for the CdS/TiO₂. Although the methanol concentration for the CdS/40 wt% TiO₂/SBA-15 was just slightly higher than that of CdS/TiO₂, the amount of TiO₂ in the CdS/40 wt% TiO₂/SBA-15 was

much lower than that of CdS/TiO₂. In this case, the methanol yield based on the amount of TiO₂ for the CdS/40 wt% TiO₂/SBA-15 could still be much higher than that of CdS/TiO₂, as shown in Fig. 4b. These results can be explained by the above textural properties. The mesoporous SBA-15 with high specific surface area and pore volume can greatly promote the mass transport and reactants adsorption. In addition, the mesoporous structure caused by the added SBA-15 may also strengthen the photon transfer in this layer, which is very propitious to the photocatalytic reaction. As a consequence, the addition of the mesoporous SBA-15 can greatly enhance the CO₂ photoreduction reaction. On the other hand, it can be seen that although the TiO₂ dosage increased from 20 wt% to 40 wt%, the methanol yield of the latter was lower than the former. The performances of the developed microreactors with these composite membranes followed the sequence of CdS/TiO₂<CdS/40wt% TiO₂/SBA-15<CdS/20 wt% TiO₂/SBA-15. The explanation of this phenomenon can refer to the BET results. In case that the TiO₂ dosage was too high, more intrinsic pores of SBA-15 were blocked by the TiO₂ nanoparticles, leading to the lowered BET surface area. Correspondingly, the pore volume was also decreased. As a result, the mass transport and reactants adsorption were hindered, while the photon transport was also resisted, both of which decreased the photocatalytic reaction rate. Therefore, the performance of the CdS/40 wt% TiO₂/SBA-15 was lower than that of the CdS/20 wt% TiO₂/SBA-15. This fact indicates that proper design of the ratio of the TiO₂ to SBA-15 is critically important to improve the photocatalytic conversion of CO₂ to solar fuels.



(a)



(b)

Fig. 4 Effect of the liquid flow rate on (a) methanol concentration and (b) methanol yield.

Besides, it can also be seen from Fig. 4a that the methanol concentration increased firstly and then decreased with increasing of the liquid flow rate. The reasons leading

to these phenomena can be presented as follows. Low liquid flow rate i.e., large residence time, allowed the reactants to take part in the photocatalytic reaction more efficiently. Hence more methanol could be produced. However, because of oxygen generated in the CO₂ photoreduction process, the generated methanol could be re-oxidized [30]. Meanwhile, the desorption of the products became slow at low flow rate and the transfer rate of the OH⁻ ion was small, which also promoted the methanol reoxidation. As a result, the methanol concentration became small at low liquid flow rate. With the increase of the liquid flow rate, although the residence time became shorter, the mass transport of the OH⁻ ion could be enhanced, which facilitated the CO₂ photoreduction reaction. On the other hand, the generated methanol could be efficiently washed away, which avoided the re-oxidation of methanol. Therefore, the methanol concentration was improved as the liquid flow rate was increased from 12.5 μL/min to 25 μL/min. However, as the liquid flow rate was further increased, the methanol concentration started to decline. Three reasons contributed to the declined methanol concentration at high liquid flow rate. First, although the mass transport could be enhanced, the increased liquid flow rate indicated small residence time, which was not beneficial for the CO₂ photoreduction to methanol. Second, an increase in the liquid flow rate means the increased liquid pressure so that more liquid phase was able to penetrate into the carbon paper. More pore space in the carbon paper might be occupied by the liquid phase, hindering the transfer of gas CO₂ from the gas microchamber to the photocatalytic film and thereby decreasing the CO₂ photoreduction rate. Third, the generated methanol could be diluted when the liquid

flow rate was increased. As a consequence, the methanol concentration was decreased as the liquid flow rate was increased from 25 $\mu\text{L}/\text{min}$ to 75 $\mu\text{L}/\text{min}$. The maximum methanol concentration was achieved at the liquid flow rate of 25 $\mu\text{L}/\text{min}$.

With the measured methanol concentration, the methanol yield M ($\mu\text{mole}/\text{g}\text{-cat}\cdot\text{h}$) was calculated according to the following equation,

$$M = \frac{60 \times c \cdot f \times 10^{-6}}{m} \quad (1)$$

where c (mmol/L) is the methanol concentration, f ($\mu\text{L}/\text{min}$) is the liquid flow rate and m (mg) is the sole TiO_2 loading. As seen in Fig. 4b, the methanol yield in all cases increased firstly and then decreased with the increase of the liquid flow rate. A maximum methanol yield was achieved at a liquid flow rate of 50 $\mu\text{L}/\text{min}$. Clearly, although high liquid flow rate benefitted for the improvement in the methanol yield indicated by Eq. (1), low methanol concentrations at both too low and too high liquid flow rates resulted in the decrease of the methanol yield. Therefore, there existed a liquid flow rate leading to the maximum methanol yield. Interestingly, the maximum methanol concentration was achieved at a liquid flow rate of 25 $\mu\text{L}/\text{min}$, while the maximum methanol yield was achieved at a liquid flow rate of 50 $\mu\text{L}/\text{min}$. This might be because the positive contribution of the increased liquid flow rate to the methanol yield was more significant than that of the decreased methanol concentration when the liquid flow rate was increased from 25 $\mu\text{L}/\text{min}$ to 50 $\mu\text{L}/\text{min}$. Hence, although the methanol concentration decreased, the methanol yield still continued to increase. Because of this reason, the liquid flow rate leading to the maximum methanol yield was shifted to 50 $\mu\text{L}/\text{min}$. More importantly, it can be found that the addition of

SBA-15 could greatly improve the methanol yield. The maximal methanol yield for the CdS/20 wt% TiO₂/SBA-15 and CdS/40 wt% TiO₂/SBA-15 could reach about 800 μmole/g-cat·h and 393 μmole/g-cat·h, respectively, which was almost four times and one time higher than that of the CdS/TiO₂, respectively. This fact further indicates that the incorporation of the mesoporous SBA-15 into the composite membrane is a promising way to improve the performance of the CO₂ photoreduction.

3.3 Effect of the light intensity

Because the CO₂ photoreduction is initiated by the photo-generated electron-hole pairs, the light intensity plays an important role in the methanol generation. Hence, it is necessary to investigate the effect of the light intensity on the performance of the optofluidic membrane microreactor with the developed composite membrane. In this study, the light intensity varied from 20 mW/cm² to 140 mW/cm², the liquid flow rate was maintained at 25 μL/min, and NaOH concentration was kept at 0.05 M. Because the xenon lamp can generate the heat to change the temperature, the change of the light intensity can affect the operating temperature of the microreactor. To remove the temperature effect, an electric fan was used to cool down the microreactor all the time to keep the microreactor temperature at room temperature. Since the CdS/20 wt% TiO₂/SBA-15 has been proved to be able to yield the best performance, we only compared the CdS/20 wt% TiO₂/SBA-15 with conventional CdS/TiO₂. The results are presented in Fig. 5, which shows that with increasing the light intensity, both the

methanol concentration and yield of the CdS/TiO₂ and CdS/20 wt% TiO₂/SBA-15 increased. More importantly, the CdS/20 wt% TiO₂/SBA-15 always yielded higher performance than did the CdS/TiO₂. It is easy to understand that high light intensity can generate more electron-hole pairs for the photocatalytic reaction. Consequently, more methanol could be generated, leading to the increase of the methanol concentration and yield. The increased methanol concentration and yield by the CdS/20 wt% TiO₂/SBA-15 can be attributed to the mesoporous structure of SBA-15, which promoted the mass transfer and adsorption and enhanced the reflection and scattering of light. Therefore, the CdS/20 wt% TiO₂/SBA-15 yielded better performance than did the CdS/TiO₂.

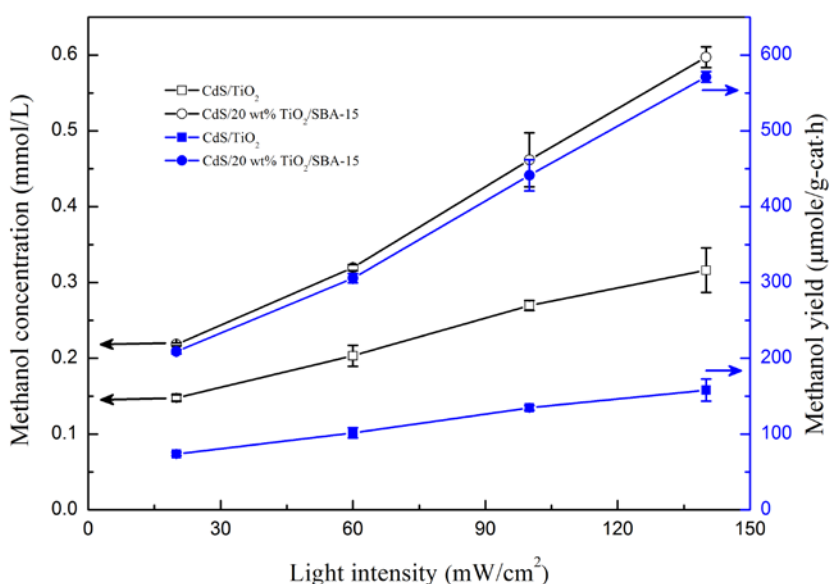


Fig. 5 Effect of light intensity on the methanol concentration and yield.

Although increasing the light intensity can improve the methanol yield, the input solar energy also increases. Hence, it is essential to evaluate the solar energy utilization efficiency. Generally, the reaction for the CO₂ photoreduction to methanol requires six moles of electrons to convert one mole CO₂ to one mole methanol [30]. In order to evaluate the solar energy utilization efficiency, the quantum efficiency (QE) was employed and given by the equation (2) and (3) [33].

$$\text{Quantum efficiency (\%)} = \frac{6 \times \text{moles of methanol yield}}{\text{moles of photon flux input}} \times 100\% \quad (2)$$

$$\text{Photon flux input} = \frac{I_{\text{int}} (\text{W/m}^2) \times A (\text{m}^2)}{hc / \lambda} \quad (3)$$

where I_{int} is the incident light intensity, A is the area of light irradiation, h is the Plank constant, c is the speed of light and λ is the wavelength of incident light. In this estimation, it is assumed that one pair of photo-generated electron-hole is generated by one photon.

Table 2 Comparison of the quantum efficiency (%) between the CdS/TiO₂ and CdS/20 wt% TiO₂/SBA-15.

Light intensity (mW/cm ²)	CdS/TiO ₂	CdS/20 wt% TiO ₂ /SBA-15
20	1.63	4.61
60	0.749	2.25
100	0.596	1.95
140	0.499	1.80

Table 2 lists the quantum efficiencies of the CdS/TiO₂ and CdS/20 wt% TiO₂/SBA-15 under different light intensities. Clearly, the increase of the light intensity decreased

the quantum efficiencies of them. As known, although more electron-hole pairs could be generated at high light intensity, more electron-hole pairs might be re-combined, leading to the lowered quantum efficiency. On the other hand, the light intensity may have been beyond the saturation limit [34], so that the increase of the light intensity was unable to improve the quantum efficiency. However, despite the quantum efficiency decreased with increasing the light intensity, the CdS/20 wt% TiO₂/SBA-15 always exhibited higher quantum efficiency than did the CdS/TiO₂. This can be contributed to the addition of SBA-15, which strengthened the photon transport and absorption as a result of enhanced the reflection and scattering of light. Therefore, the addition of SBA-15 can improve not only the methanol yield but also the quantum efficiency.

3.4 Effect of the NaOH concentration

As presented before, the addition of NaOH was because it could increase the CO₂ solubility and CdS stability and prevent the recombination of the electron-hole pairs. Therefore, the performance of the optofluidic membrane microreactor with the developed composite membrane can be greatly affected by the NaOH concentration, whose effect was then investigated in this study. To do this, the liquid flow rate was kept at 25 μ L/min, and the light intensity was maintained at 100 mW/cm², while the NaOH concentration ranged from 0.05 M to 0.4 M. As shown in Fig. 6, an increase in the NaOH concentration led to the increase of the methanol concentration and yield for both the CdS/TiO₂ and CdS/20wt% TiO₂/SBA-15. It is clear that the increased

NaOH concentration not only improved the CO₂ solubility, which was helpful for the methanol generation, but also resisted the recombination of the electron-hole pairs, which definitely enhanced the CO₂ photoreduction. More importantly, it can be seen that the CdS/20wt% TiO₂/SBA-15 always yielded better performance than did the CdS/TiO₂. Increasing the NaOH concentration from 0.05 M to 0.4 M resulted in an increase in the methanol concentration and yield for both CdS/TiO₂ and CdS/20wt% TiO₂/SBA-15. The improvement in the performance with increasing the NaOH concentration can be explained in terms of the enhancement of the CO₂ solubility into the solution and the recombination of photo-generated electron-hole pairs were hindered efficiently. It is also clear that a much higher methanol yield of CdS/20wt% TiO₂/SBA-15 was obtained than pure CdS/TiO₂, which thanks to the OH⁻ ions served as holes scavengers. With the mesoporous SBA-15, the transport of the OH⁻ ion can be greatly enhanced so that much more hydroxyl radicals can be formed on the photocatalysts. As a result, the methanol generation by the CO₂ photoreduction can be improved. On the other hand, it has been revealed that a higher selectivity for the methanol formation with TiO₂ based mesoporous photocatalysts was achieved [16], which was also favorable for the performance improvement. Because of these reasons, the CdS/20 wt% TiO₂/SBA-15 exhibited better methanol yield. A maximum methanol yield of about 1022 μmole/g-cat·h was obtained at 0.4 M NaOH concentration, which was nearly 4 times higher than CdS/TiO₂. In summary, higher NaOH concentration is beneficial for the CO₂ photoreduction and the incorporation of SBA-15 shows the advantageous performance than conventional CdS/TiO₂.

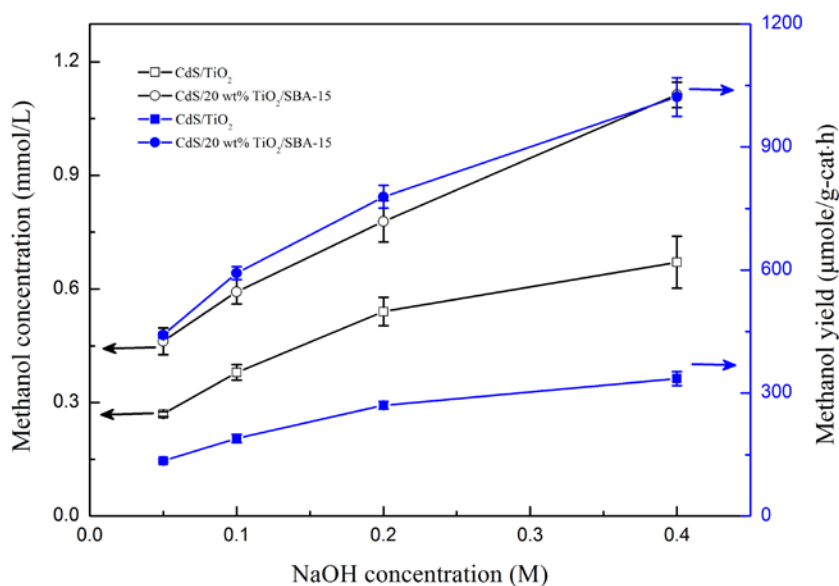


Fig. 6 Effect of the NaOH concentration on the methanol concentration and yield.

4. Conclusions

In this work, a CdS/TiO₂/SBA-15@carbon paper composite membrane was developed for the optofluidic membrane microreactor toward the CO₂ photoreduction with the visible-light response. In addition to the merits provided by the optofluidic platform, the incorporation of mesoporous SBA-15 into the composite membrane could provide large specific surface area and pore volume, enhance light scattering and facilitate the mass and photon transport inside the catalytic layer. Because of these advantages, the optofluidic membrane microreactor with the CdS/TiO₂/SBA-15@carbon paper composite membrane yielded better performance than did with the conventional composite membrane. It was also found that too high TiO₂ dosage in the composite membrane could result in the lowered performance because a significant amount of meso pores and macro pores might be blocked by the

TiO₂ nanoparticles. In addition, the effects of the operating conditions, including the liquid flow rate, light intensity and NaOH concentration were also studied. It was shown that both the methanol concentration and yield firstly increased and then decreased with increasing the liquid flow rate. Meanwhile, increasing the light intensity and NaOH concentration could result in the improvement in the methanol concentration and yield because of more photo-generated electron-hole pairs and OH⁻ ions served as hole scavengers. The obtained results have fully demonstrated that the incorporation of mesoporous materials into the optofluidic membrane microreactor shows promising perspective for the CO₂ photoreduction to solar fuels. Such design can also be applied to other photochemical systems such as wastewater treatment, water-splitting and so on.

Acknowledgements

The authors gratefully acknowledge the financial supports of the National Natural Science Foundation of China (No. 51576021, No.51276208 and No.51325602), the National High Technology Research and Development Program of China (863 Program) (No. 2015AA043503) and the Fundamental Research Funds for the Central Universities (No. CDJZR14145502).

Reference

- [1] D.Y.C. Leung, G. Caramanna, M.M. Maroto-Valer, An overview of current status of carbon dioxide capture and storage technologies, *Renewable Sustainable Energy Rev* 39 (2014) 426-443.
- [2] Y.H. Cheng, V.H. Nguyen, H.Y. Chan, J.C.S. Wu, W.H. Wang, Photo-enhanced hydrogenation of CO₂ to mimic photosynthesis by CO co-feed in a novel twin reactor, *Appl. Energy* 147 (2015) 318-324.
- [3] C.C. Wang, Y.Q. Zhang, J. Li, P. Wang, Photocatalytic CO₂ reduction in metal-organic frameworks: a mini review, *J. Mol. Struct* 1083 (2015) 127-136.
- [4] X.X. Chang, T. Wang, J.L. Gong, CO₂ Photo-reduction: Insights into CO₂ Activation and Reaction on Surfaces of Photocatalysts, *Energy Environ. Sci.* 9 (2016) 2177-2176.
- [5] K. Li, X. An, K.H.P. Park, M. Khraisheh, J.W. Tang, A critical review of CO₂ photoconversion: catalysts and reactors, *Catal. Today* 224 (2014) 3-12.
- [6] O. Ola, M.M. Maroto-Valer, Review of material design and reactor engineering on TiO₂ photocatalysis for CO₂ reduction, *J. Photochem. Photobiol. C* 24 (2015) 16-42.
- [7] W. Tu, Y. Zhou, Z. Zou, Photocatalytic Conversion of CO₂ into Renewable Hydrocarbon Fuels: State-of-the-Art Accomplishment, Challenges, and Prospects, *Adv. Mater.* 26 (2014) 4607-4626.
- [8] A. Dhakshinamoorthy, S. Navalon, A. Corma, H. Garcia, Photocatalytic CO₂ reduction by TiO₂ and related titanium containing solids, *Energy Environ. Sci* 5 (2012)

9217-9233.

[9] S. Das, W.M.A.W. Daud, Photocatalytic CO₂ transformation into fuel: A review on advances in photocatalyst and photoreactor, *Renewable Sustainable Energy Rev* 39 (2014) 765-805.

[10] C. Salameh, J. P. Nogier, F. Launay, M. Boutros, Dispersion of colloidal TiO₂ nanoparticles on mesoporous materials targeting photocatalysis applications, *Catal. Today* 257 (2015) 35-40.

[11] H.H. Tseng, W.W. Lee, M.C. Wei, B.S. Huang, M.C. Hsieh, P.Y. Cheng, Synthesis of TiO₂/SBA-15 photocatalyst for the azo dye decolorization through the polyol method, *Chem. Eng. J.* 210 (2012) 529-538.

[12] C.Y. Zhao, L.J. Liu, Q.Y. Zhang, J. Wang, Y. Li, Photocatalytic conversion of CO₂ and H₂O to fuels by nanostructured Ce-TiO₂/SBA-15 composites, *Catal. Sci. Technol.* 2 (2012) 2558-2568.

[13] L. Lin, R. Chen, X. Zhu, Q. Liao, H. Wang, L. An, M.X. Zhang, A cascading gradient pore microstructured photoanode with enhanced photoelectrochemical and photocatalytic activities, *J. Catal.* 344 (2016) 411-419.

[14] J. Yang, J. Zhang, L.W. Zhu, S.Y. Chen, Y.M. Zhang, Y. Tang, Y.L. Zhu, Y.W. Li, Synthesis of nano titania particles embedded in mesoporous SBA-15: characterization and photocatalytic activity, *J. Hazard. Mater.* 137 (2006) 952-958.

[15] X.H. Li, W.L. Zheng, H.Y. Pan, Y. Yu, L. Chen, P. Wu, Pt nanoparticles supported on highly dispersed TiO₂ coated on SBA-15 as an efficient and recyclable catalyst for liquid-phase hydrogenation, *J. Catal.* 300 (2013) 9-19.

- [16] H.C. Yang, H.Y. Lin, Y.S. Chien, J.C.S. Wu, H.H. Wu, Mesoporous TiO₂/SBA-15, and Cu/TiO₂/SBA-15 composite photocatalysts for photoreduction of CO₂ to methanol, *Catal. Lett.* 131 (2009) 381-387.
- [17] M. Tahir, N.A.S. Amin, Advances in visible light responsive titanium oxide-based photocatalysts for CO₂ conversion to hydrocarbon fuels, *Energy Convers. Manage.* 76 (2013) 194-214.
- [18] D. Zhao, C.F. Yang, Recent advances in the TiO₂/CdS nanocomposite used for photocatalytic hydrogen production and quantum-dot-sensitized solar cells, *Renew. Sust. Energ. Rev.* 54 (2016) 1048-1059.
- [19] P.S. Lunawat, R. Kumar, N.M. Gupta, Structure sensitivity of nano-structured CdS/SBA-15 containing Au and Pt co-catalysts for the photocatalytic splitting of water, *Catal. Lett.* 121 (2008) 226-233.
- [20] L. Li, R. Chen, Q. Liao, X. Zhu, G.Y. Wang, D.Y. Wang, High surface area optofluidic microreactor for redox mediated photocatalytic water splitting, *Int. J. Hydrogen. Energy* 39 (2014) 19270-19276.
- [21] L. Li, R. Chen, X. Zhu, H. Wang, Y.Z. Wang, Q. Liao, D.Y. Wang, Optofluidic microreactors with TiO₂-coated fiberglass, *ACS Appl. Mater. Inter.* 5 (2013) 12548-12553.
- [22] X. Cheng, R. Chen, X. Zhu, Q. Liao, L. An, D.D. Ye, X.F. He, S.Z. Li, L. Li, An optofluidic planar microreactor for photocatalytic reduction of CO₂ in alkaline environment, *Energy*, DOI: 10.1016/j.energy.2016.11.081
- [23] J.L.H. Chau, A.Y.L. Leung, K.L. Yeung, Zeolite micromembranes, *Lab Chip* 3

(2003) 53-55.

[24] W.N. Lau, K.L. Yeung, R. Martin-Aranda, Knoevenagel condensation reaction between benzaldehyde and ethyl acetoacetate in microreactor and membrane microreactor, *Microporous Mesoporous Mater.* 115 (2008) 156-163.

[25] M. Liu, X. Zhu, R. Chen, Q. Liao, H. Feng, L. Li, Catalytic membrane microreactor with Pd/ γ -Al₂O₃ coated PDMS film modified by dopamine for hydrogenation of nitrobenzene, *Chem. Eng. J.* 301 (2016) 35-41.

[26] X. Cheng, R. Chen, X. Zhu, Q. Liao, X.F. He, S.Z. Li, L. Li, Optofluidic membrane microreactor for photocatalytic reduction of CO₂, *Int. J. Hydrogen Energy.* 4 (2016) 2457-2465.

[27] F. Bresciani, C. Rabissi, M. Zago, P. Gazdzicki, M. Schulze, L. Guetaz, S. Escribano, J.L. Bonde, R. Marchesi, A. Casalegno, A combined in-situ and post-mortem investigation on local permanent degradation in a direct methanol fuel cell, *J. Power Sources* 306 (2016) 49-61.

[28] M. Antoniadou, D.I. Kondarides, D.D. Dionysiou, P. Lianos, Quantum dot sensitized titania applicable as photoanode in photoactivated fuel cells, *J. Phys. Chem. C* 116 (2012) 16901-16909.

[29] Y. Zhao, L. Xu, Y.Z. Wang, C.G. Gao, D.S. Liu, Preparation of Ti-Si mixed oxides by sol-gel one step hydrolysis, *Catal. Today* 93 (2004) 583-588.

[30] I.H. Tseng, W.C. Chang, J.C.S. Wu, Photoreduction of CO₂ using sol-gel derived titania and titania-supported copper catalysts, *Appl. Catal., B* 37 (2002) 37-48.

- [31] V.M. Daskalaki, M. Antoniadou, G.L. Puma, D.I. Kondarides, P. Lianos, Solar light-responsive Pt/CdS/TiO₂ photocatalysts for hydrogen production and simultaneous degradation of inorganic or organic sacrificial agents in wastewater, *Environ. Sci. Technol.* 44 (2010) 7200-7205.
- [32] Y. Shioya, K. Ikeue, M. Ogawa, M. Anpo, Synthesis of transparent Ti-containing mesoporous silica thin film materials and their unique photocatalytic activity for the reduction of CO₂ with H₂O, *Appl. Catal. A* 254 (2003) 251-259.
- [33] W.H. Lee, C.H. Liao, M.F. Tsai, C.W. Huang, J.C.S. Wu, A novel twin reactor for CO₂ photoreduction to mimic artificial photosynthesis, *Appl. Catal., B* 132 (2013) 445-451.
- [34] J.C.S. Wu, T.H. Wu, T.C. Chu, H.J. Huang, D.P. Tsai, Application of optical-fiber photoreactor for CO₂ photocatalytic reduction, *Top. Catal.* 47 (2008) 131-136.